Zero-strain $Ca_{0.4}Ce_{0.6}VO_4$ Anode Material for High Capacity and Long-Life Na-Ion Batteries

Guisheng Liang[a,b], Xuhui Xiong[b], Liting Yang[b], Xianhu Liu[c], Renchao Che[a,b]*

[a.] *Materials Genome Institute, Shanghai University, Shanghai 200444, China*

[b.] *Laboratory of Advanced Materials, Shanghai Key Lab of Molecular Catalysis and Innovative Materials, Fudan University, Shanghai 200438, P. R. China*

[c.] *School of Materials Science and Engineering, National Engineering Research Center for Advanced Polymer Processing Technology, Henan Province Industrial Technology Research Institute of Resources and Materials, Key Laboratory of Advanced Material Processing & Mold (Ministry of Education), Zhengzhou University, Zhengzhou, 450002, China*

Table S1. The XRD Rietveld refinement results of $CeVO_4$.

$CeVO_4$ (tetragonal, *I41/amd*)					
R_p = 10.9% R_{wp} = 14.9% R_{exp} = 10.18% Chi2 = 2.14					
$a = b = 7.40115$ Å, $c = 6.50005$ Å, $\alpha = \beta = \gamma = 90°$, $V = 356.054$ Å^3					
Atoms	***x***	***y***	***z***	**sites**	**Occupation**
Ce1	0.00000	0.75000	0.12500	4a	1.000
V1	0.00000	0.25000	0.37500	4b	1.000
O1	0.00000	0.42830	0.20660	16h	1.000

Table S2. The XRD Rietveld refinement results of Ca-$CeVO_4$.

Ca-$CeVO_4$ (tetragonal, *I41/amd*)					
R_p = 10.4% R_{wp} = 13.6% R_{exp} = 11.09% Chi2 = 1.50					
$a = b = 7.23940$ Å, $c = 6.40983$ Å, $\alpha = \beta = \gamma = 90°$, $V = 335.932$ Å^3					
Atoms	***x***	***y***	***z***	**sites**	**Occupation**
Ca1	0.00000	0.75000	0.12500	4a	0.400
Ce1	0.00000	0.75000	0.12500	4a	0.600
V1	0.00000	0.25000	0.37500	4b	1.000
O1	0.00000	0.56852	0.801250	16h	1.000

Table S3. Mean elemental composition in weight% obtained by ICP-OES $CeVO_4$ and $Ca_{0.4}Ce_{0.6}VO_4$.

sample	Ca content (%)	Ce content (%)	V content (%)
$CeVO_4$	–	56.3	20.0
$Ca_{0.4}Ce_{0.6}VO_4$	7.4	39.1	23.7

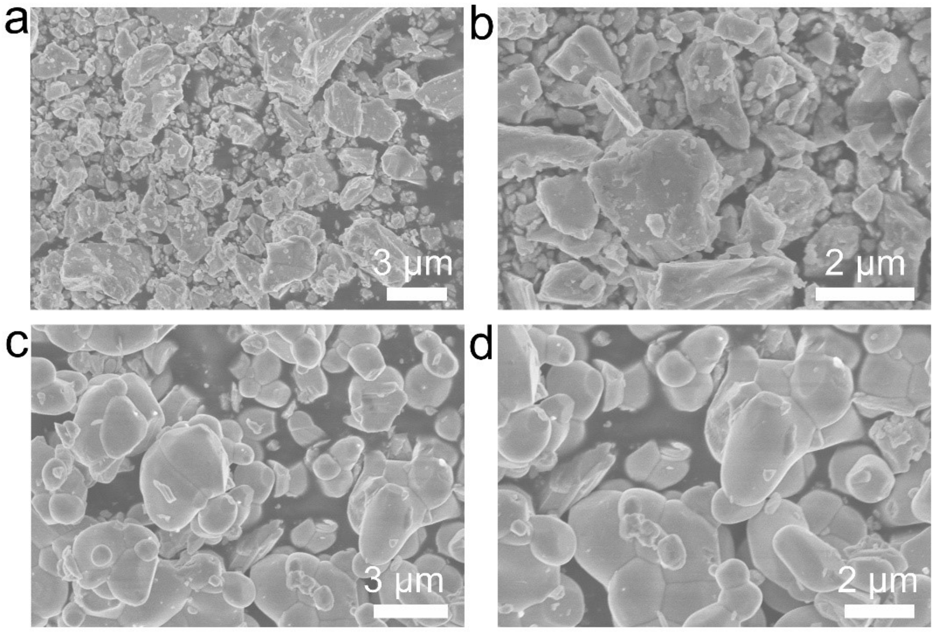

Fig. S1. FESEM images of (a, b) Ca-$CeVO_4$ and (c,d) $CeVO_4$.

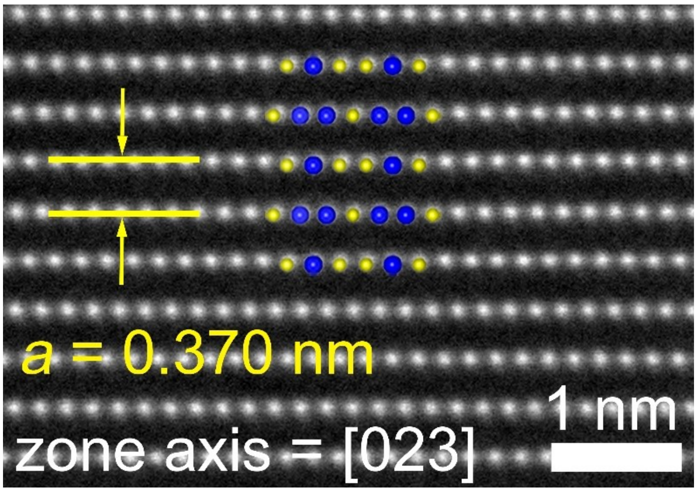

Fig. S2. HAADF STEM images of $CeVO_4$. The Ce and V atoms are colored by blue and yellow, respectively.

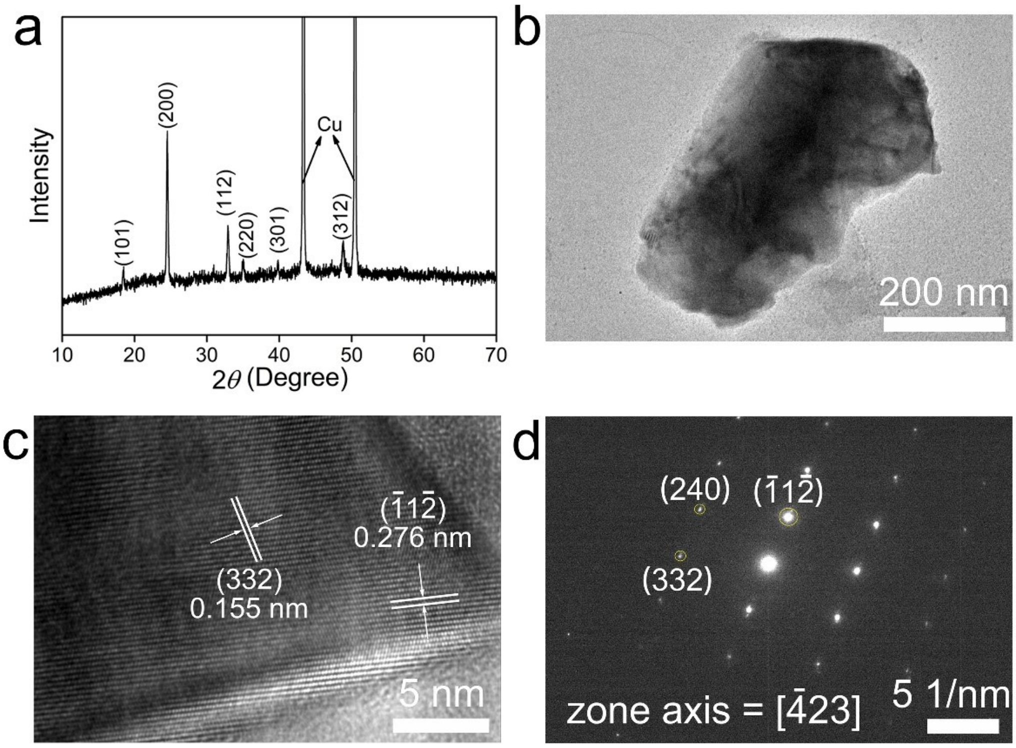

Fig. S3. *Ex-situ* (a) XRD pattern, (b) FETEM image and (c) HRTEM image and SAED pattern of Ca-$CeVO_4$ after long-term cycling. The tested Ca-$CeVO_4$ sample was obtained through disassembling Ca-$CeVO_4$/Na half cell after 2000 cycles at 1500 mA g^{-1}.

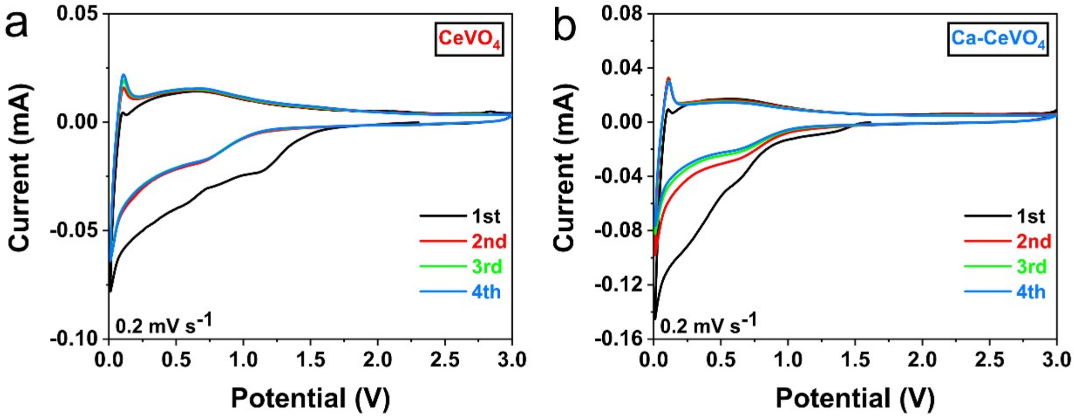

Fig. S4. The original four CV curves of **(a)** $CeVO_4$ and **(b)** Ca-$CeVO_4$.

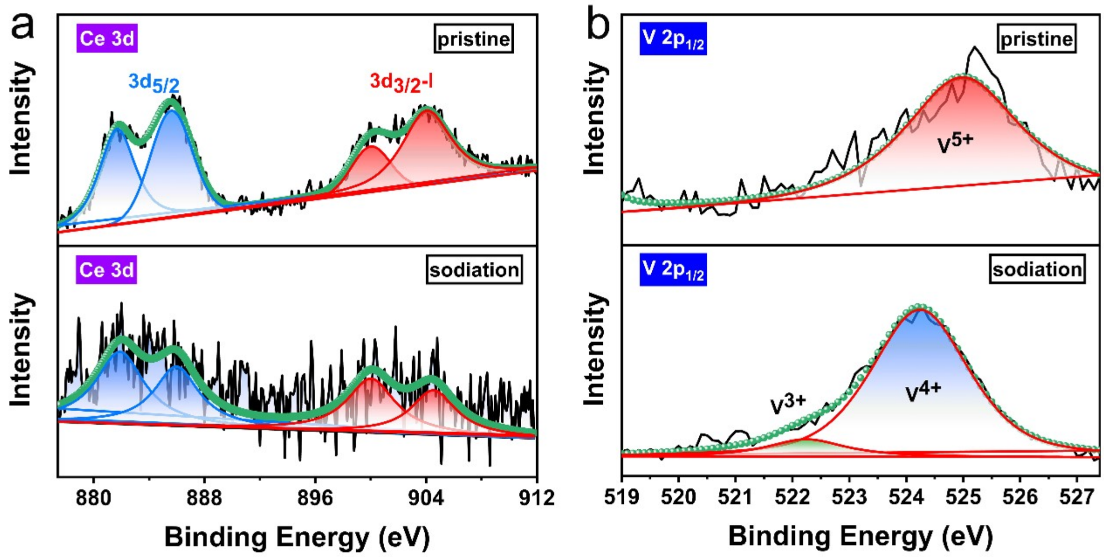

Fig. S5. The **(a)** Ce 3d and **(b)** V $2p_{1/2}$ XPS spectra of $CeVO_4$ in different sodiation states.

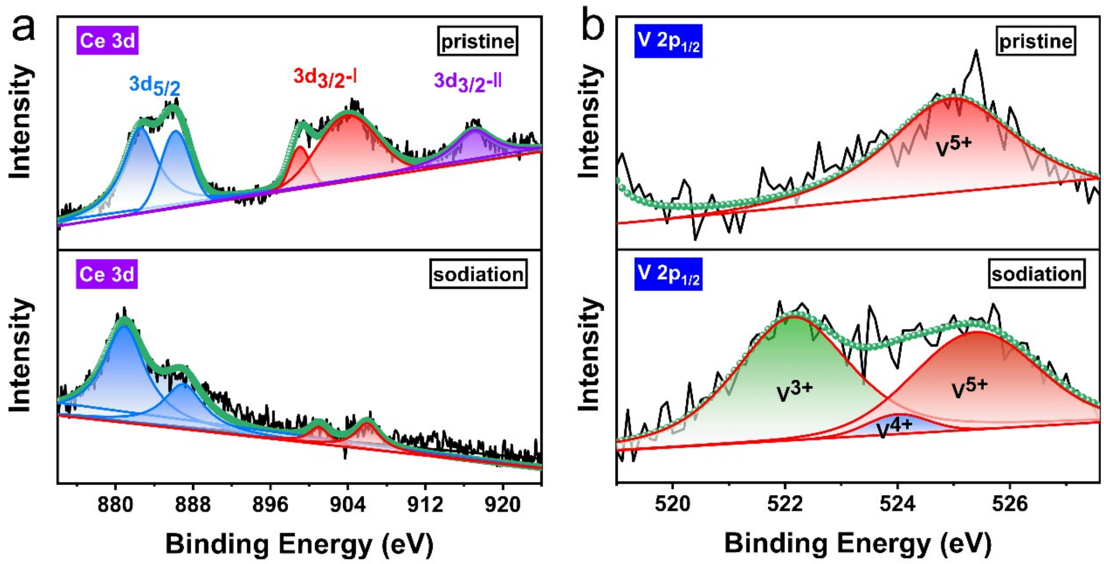

Fig. S6. The **(a)** Ce 3d and **(b)** V $2p_{1/2}$ XPS spectra of Ca-$CeVO_4$ in different sodiation states.

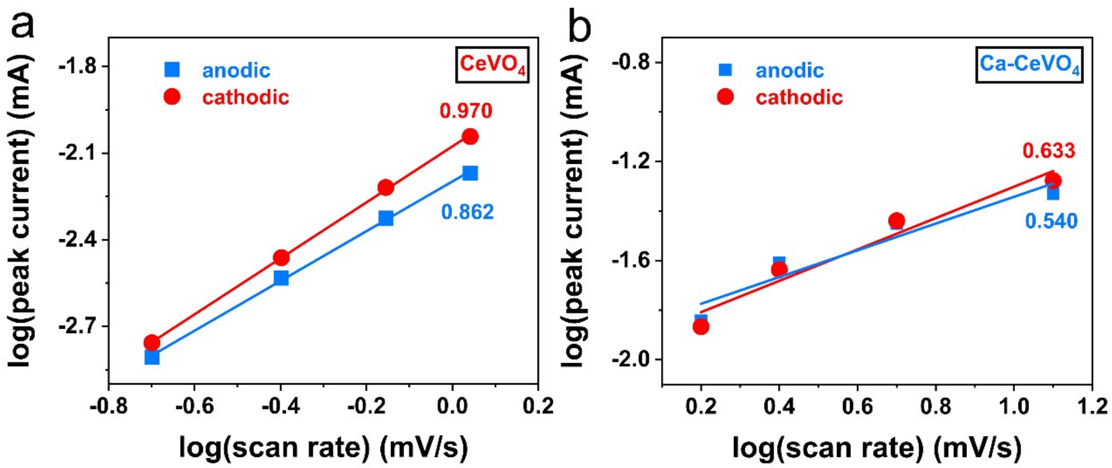

Fig. S7. The function with log (peak current) *vs.* log (scan rate) for **(a)** $CeVO_4$ and **(b)** Ca-$CeVO_4$, which is used to determine the value of b.

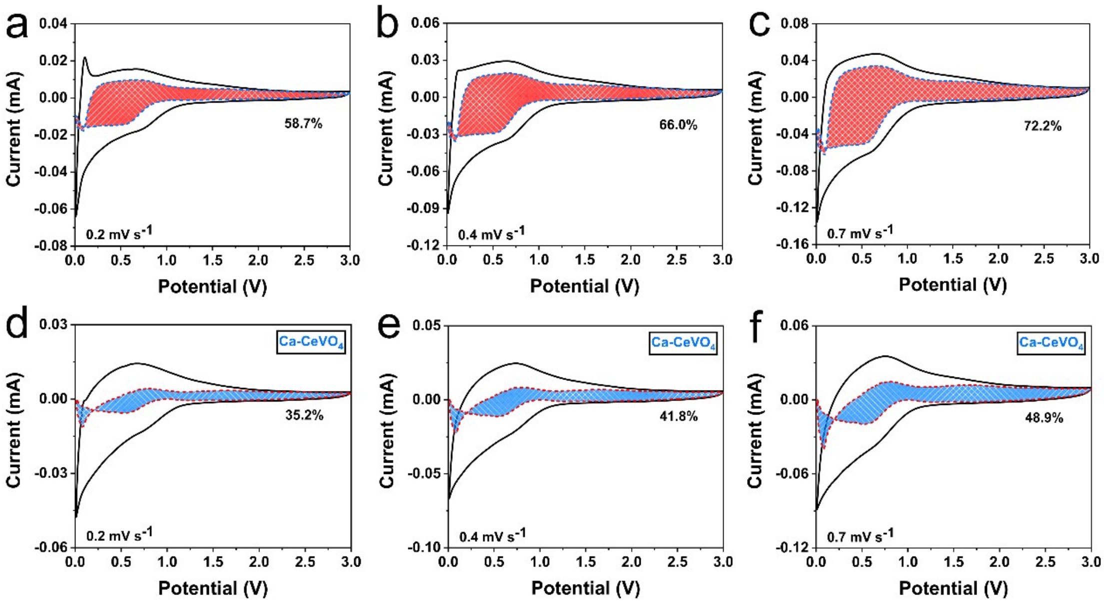

Fig. S8. The detailed CV curves with pseudocapacitive contribution at the scan rates of 0.2, 0.4 and 0.7 mV s^{-1}. **(a, b, c)** $CeVO_4$. **(d, e, f)** Ca-$CeVO_4$.

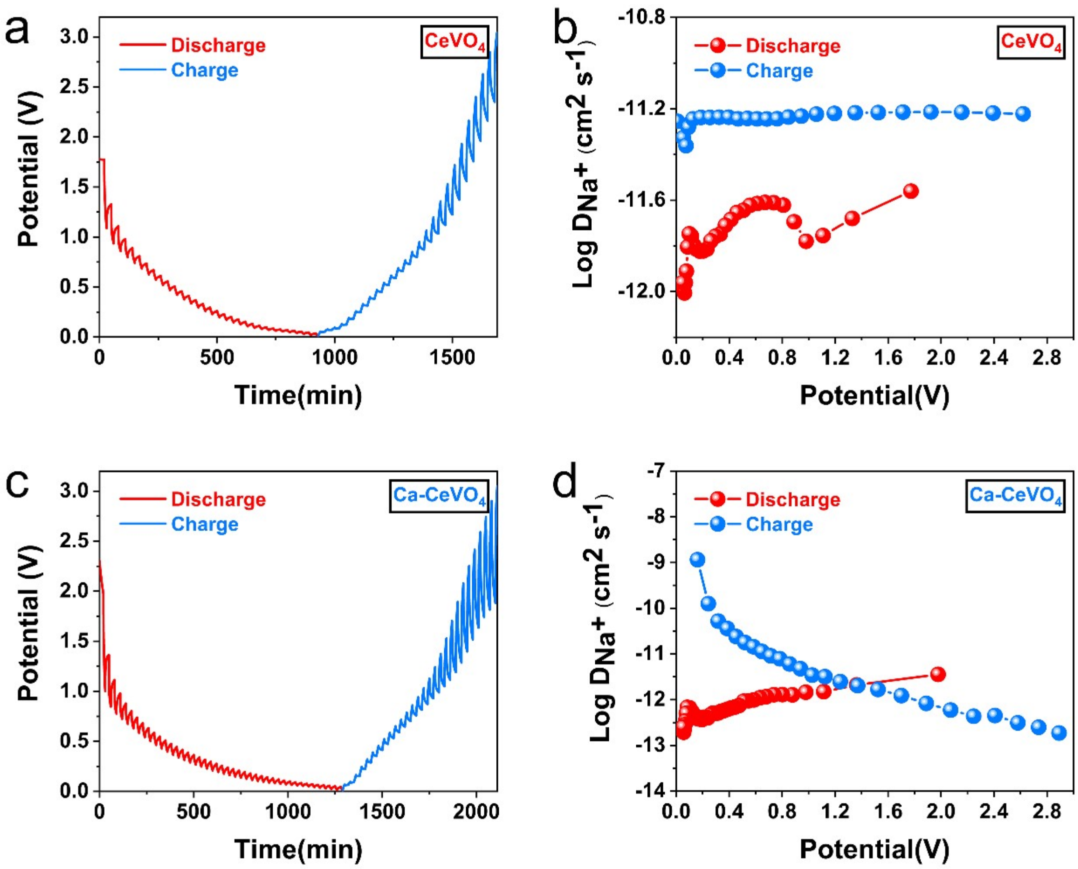

Fig. S9. The evaluating of Li^+ diffusion coefficients based on GITT experiments in $CeVO_4$ and Ca-$CeVO_4$. (a, b) GITT curves during the process of discharging and charging. **(c, d)** The logarithm of calculated Na^+ diffusion coefficients (log D_{Na}) changes with the potential (V).

The GITT experiments were also applied to investigate the Na^+ diffusion coefficient (D_{Na}) of Ca-$CeVO_4$ and $CeVO_4$ (**Fig. S8**). The times of pulse and intermittence are selected as 10 min and 20 min, respectively (**Fig. S9a and c**). According to the previous reports, the D_{Na} in can be determined based on the second Fick's law, as described in **Eq. (S1) and (S2)**[S1-S4]

$$D_{Na} = \frac{4}{\pi}\left(\frac{m_B V_m}{M_B S}\right)^2 \left(\frac{\Delta E_s}{\tau (dE_\tau / d\sqrt{\tau})}\right)^2 \quad \left(\tau \ll \frac{L^2}{D}\right) \tag{S1}$$

$$D_{Na} = \frac{4}{\pi\tau}\left(\frac{m_B V_m}{M_B S}\right)^2 \left(\frac{\Delta E_s}{\Delta E_\tau}\right)^2 \ \left(\tau \ll \frac{L^2}{D}\right) \tag{S2}$$

where m_B, V_m, M_B and S is the active materials mass, molar volume, molar mass and electrode contact area, respectively. ΔE_τ and ΔE_s represents the potential variation during a single pulse stage and the potential difference between two equilibrium states, respectively. As displayed in **Fig. S9b and d**, the potential during a single pulse process can be fitted to $\tau^{0.5}$ with a linear function, thus the simplified expression of **Eq.(S2)** can be used for calculating the Na^+ diffusion coefficients more conveniently. The average Na^+ diffusion coefficient of $CeVO_4$ and Ca-$CeVO_4$ is 3.77×10^{-12} $cm^2\ s^{-1}$ and 7.18×10^{-12} $cm^2\ s^{-1}$, respectively.

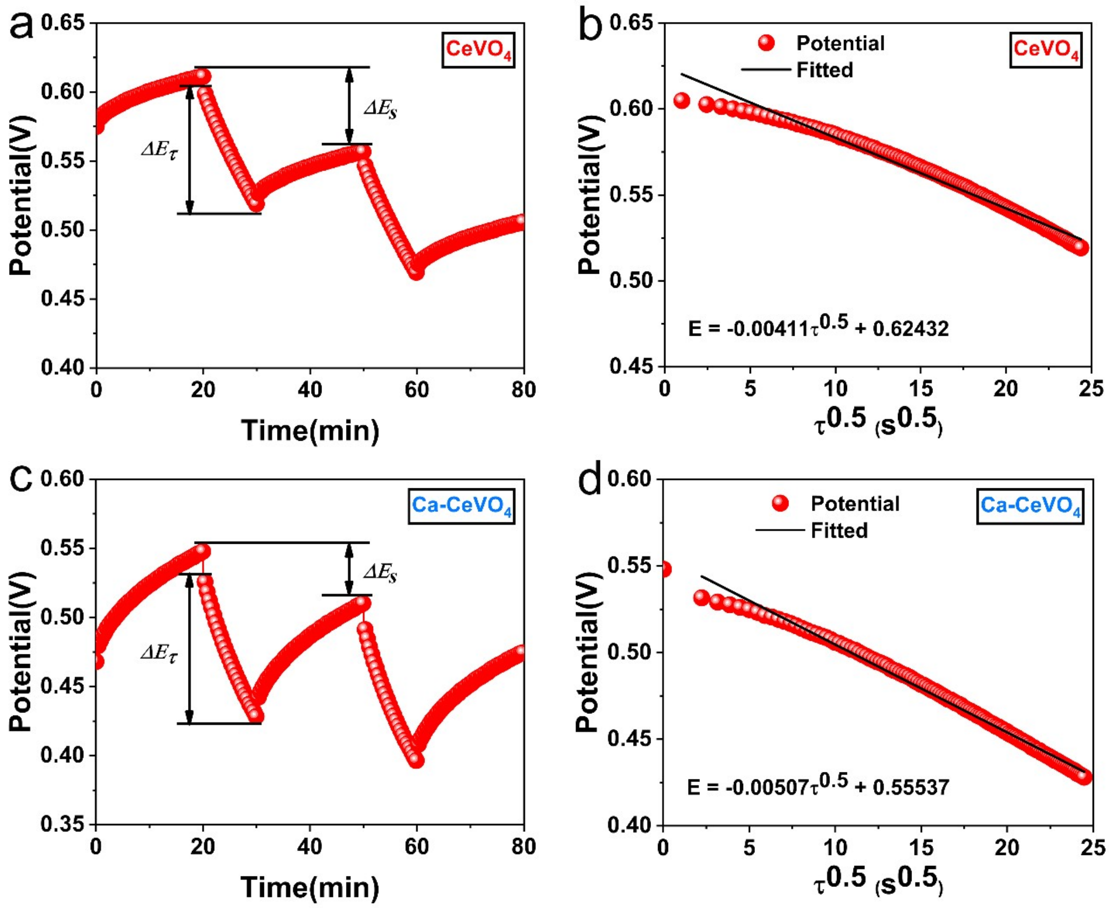

Fig. S10. The details the GITT curves of $CeVO_4$ and Ca-$CeVO_4$. (a, c) The partial enlarged detail, in which ΔE_τ represents the potential variation during a single pulse stage and ΔE_s represents the potential difference between two equilibrium states. **(b, d)**

The functional relationship between potential and $\tau^{0.5}$ (τ is the symbolization of single pulse time).

Reference

S1 W. Weppner, *J. Electrochem. Soc.*, 1977, **124**, 1569.

S2 X. Zhu, H. Cao, R. Li, Q. Fu, G. Liang, Y. Chen, L. Luo, C. Lin and X. S. Zhao, *J. Mater. Chem. A*, 2019, **7**, 25537.

S3 Z Hong, Y. Zhen, Y. Ruan, M. Kang, K. Zhou, J. M. Zhang, Z. Huang and M. Wei, *Adv. Mater.*, 2018, 1802035.

S4 A. J. Bard, L. R. Fa Ulkner, *Student Solutions Manual*, 2nd Edition.